Near-Unity Quantum Yield in Semiconducting Nanostructures: Structural Understanding Leading to Energy Efficient Applications

ARTICLE *in* JOURNAL OF PHYSICAL CHEMISTRY LETTERS · OCTOBER 2013

Impact Factor: 7.46 · DOI: 10.1021/jz401958u

6 AUTHORS, INCLUDING:

Avijit Saha
Jawaharlal Nehru Centre for Advanced Scienti…
2 PUBLICATIONS **18** CITATIONS
SEE PROFILE

Kishore V Chellappan
AMOS, Belgium
10 PUBLICATIONS **235** CITATIONS
SEE PROFILE

Ks Narayan
Jawaharlal Nehru Centre for Advanced Scienti…
154 PUBLICATIONS **1,719** CITATIONS
SEE PROFILE

Ranjan Datta
Jawaharlal Nehru Centre for Advanced Scienti…
78 PUBLICATIONS **1,584** CITATIONS
SEE PROFILE

THE JOURNAL OF PHYSICAL CHEMISTRY Letters

Letter

pubs.acs.org/JPCL

Near-Unity Quantum Yield in Semiconducting Nanostructures: Structural Understanding Leading to Energy Efficient Applications

Avijit Saha,[†] Kishore V. Chellappan,[‡] K. S. Narayan,[‡] Jay Ghatak,[§] Ranjan Datta,[‡,§] and Ranjani Viswanatha*[,†,§]

[†]New Chemistry Unit, [‡]Chemistry and Physics of Materials Unit, and [§]International Centre for Materials Science, Jawaharlal Nehru Centre for Advanced Scientific Research, Jakkur, Bangalore 560064, India

Supporting Information

ABSTRACT: Core/shell nanocrystal quantum dots (NQDs) have shown great potential as efficient electroluminescent materials in devices like down-conversion phosphors and light-emitting diodes (LEDs). The efficiency of these devices is nonlinearly enhanced by the use of high quantum yield (QY) materials. Though relatively high QY materials with inherent advantages for use in device applications are achieved by thick-shell CdSe/CdS NQDs, their QY is not anywhere near unity due to lack of correlation of the microstructure with their photophysical properties. Here, in this Letter, we show that the control of interfacial defects is crucial to achieve a near-unity QY using microstructure studies of CdSe/CdS NQDs. Simple unoptimized LEDs obtained from these NQDs as the active layer demonstrate performances in excess of 7000 Cd/m^2 with a power conversion efficiency of ∼1.5 lm/W that is comparable to those of the best NQD-based LEDs (1−3%) despite the absence of an electron-injecting buffer layer.

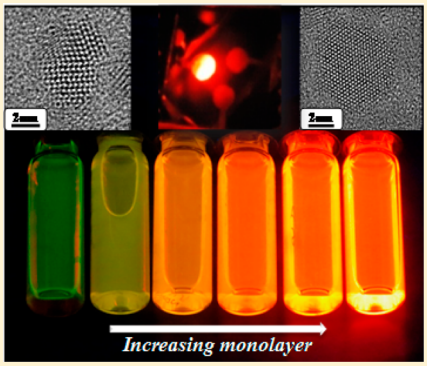

SECTION: Physical Processes in Nanomaterials and Nanostructures

Structural engineering of semiconducting nanocrystals has shown a lot of potential in improving various properties of the nanocrystals, specifically the optical properties,[1−4] for example, the growth of a higher band gap shell material is known to be extensively used to passivate the core, leading to high quantum yield (QY) structures.[5] The high photoluminescence[6] (PL) QY without electric-field-induced charging in nanocrystal quantum dots (NQDs) is a trade-off between the surface defects[7] and the core−shell interface.[8] However, among the multitude of methods available to obtain such core/shell[9] structures, the properties of the final materials obtained depend sensitively on various factors like the actual total coverage of the shell and if all nanocrystals are equally coated in addition to defects on the surface and/or at the shell interface.[8,10,11] Besides the lattice mismatch between the core and shell materials that is known to play an important role in the design of robust core/shell NQDs, in most cases, the optical properties are mainly dominated by surface defects.[7,8] Recently, this frustrating dependence of optical properties on surface chemistry and chemical environment was overcome by the growth of an ultrathick inorganic shell of CdS over CdSe core particles.[12−15] Surprisingly, these particles not only were found to rid the dots of the detrimental effects of the labile nature of organic ligands but were also shown to suppress a more intrinsic phenomenon, known as Auger recombination,[13,16−18] believed to give rise to blinking in NQDs.[12,15,19,20] Since then, various advantages inherent in these ultrathick-shell Auger-engineered CdSe/CdS NQDs have been extensively studied and have justifiably drawn a lot of attention as prospective lasing materials,[17] efficient electroluminescent materials,[21] and stable down-conversion phosphors.[22,23] In the last couple of years, the properties of these compounds have been extensively studied starting from blinking statistics[15,19] to the photostability to optical gain performance[17] as well as demonstration of LEDs.[21,23] Due to the large number of potential applications, modifying the chemistry in an effort to further optimize the QY is underway.[24] However, despite a large effort, though incremental improvements in QY are reported, not surprisingly, the recipe for a high QY material is unknown. Specifically, the QYs of these thick-shell compounds have not improved much more than 30% except in a few rare cases leading up to 50%, though high QY in thinner-shell materials is now routine.[25] However, despite the fact that the NQDs of single-material or core/shell structures with a thin-shell material have shown a close to near-unity QY,[25] the efficiency of devices has not improved substantially.

The latest efforts along this direction have attributed the low QY to the poor control of the crystal structure resulting in wurtzite rather than zinc-blende structure.[26] However, several fundamental theoretical studies on the electronic structure have emphasized that the crucial component is to suppress the Auger recombination in these materials. Calculations have shown that smoothening out the confinement potential reduces the efficiency of the Auger processes in low-dimensional hetero-

Received: September 12, 2013
Accepted: October 4, 2013
Published: October 4, 2013

   dx.doi.org/10.1021/jz401958u | J. Phys. Chem. Lett. 2013, 4, 3544−3549

structures[27] by several orders of magnitude compared to that in structures with abrupt boundaries and hence improves the QY.[27−29] Since then, extended efforts have shown that it is nontrivial to translate such a theoretical demand to materials, specifically in a uniform defect-free manner, that would lead to nanocrystals with excellent photophysical properties. Though it is well-known that the effects of a single defect[7] or interface[27] on the properties of NQDs could have far-reaching consequences due to the high defect density, the control of defects in NQDs is very challenging as a result of the large number of thermodynamic and kinetic factors involved.

Our studies in this direction have shown that the lack of a logical understanding and correlation of the microstructure with the photophysical properties of these core/shell structures is responsible for the sustained absence of high QY materials. In this Letter, we report for the first time an experimental correlation of the evolution of defects in NQDs to their photophysical properties. The control and minimization/elimination of the defects at the core−shell interface in CdSe/CdS NQDs lead to Auger-engineered[13,17] highly emissive QDs with excellent optical properties of near-unity QY. In the case of CdSe/CdS, a lattice mismatch of 3.9% between CdSe and CdS poses a serious challenge in controlling defects at the interface of the core−shell during the synthesis of a thick uniform shell. Defect-free graded alloy at the interface was achieved using a counterintuitive approach of a highly surface defective core that is demonstrated using PL lifetime studies and high-resolution microscopy. This work shows that this unusual observation can not only be explained using the well-studied sharp/smooth interface model, but a direct correlation between the QY and number of defective particles has been established by studying samples with varying QY. This is realized by a very counter-intuitive mechanism of decreasing defect density and contradictory to the expected belief, high-quality cores with low or nil surface defects are not ideally suited to yield high QY core/shell particles even in low lattice mismatch core and shell materials. In fact, we show that cores with a large number of surface defects are better suited to obtain high QY materials.

Further, the advantages of these NQDs could be directly translated into device performance in the LED. A proof-of-concept verification of device efficiency was carried out by fabricating a simple LED using near-unity QY nanocrystals as the active layer. As anticipated, the performance of these unoptimized simple devices was comparable to that of the best NQD-based LED devices (1−3%) despite the absence of an electron-injecting buffer layer. The devices retained all of the advantages of the earlier devices like remarkably low turn-on voltage in addition to the possibility of driving the device to yield luminance in the range of 7000 Cd/m^2. The sizable luminance at low input power leading to efficient devices (∼1.5 lm/W) is comparable to the efficiency of that obtained for solution-processed LEDs, 2.4 lm/W for cross-linked colloidal dots[30] and 4.2 lm/W for a transfer-printed LED.[31]

The 3 nm cores of wurtzite nanocrystals were synthesized using different concentrations of surface ligands (Table 1) and overcoated with sequential addition of Cd and S precursors, giving rise to thick-shell wurtzite CdSe/CdS nanocrystals. They were characterized using high-resolution transmission electron microscopy (HRTEM), X-ray diffraction (XRD), as well as absorption and fluorescence (Supporting Information Figure S1).

Table 1. Influence of Ligand Concentration on Average Lifetime

core	TOPO (mmol)	OlAm (mmol)	TOP (mmol)	avg. lifetime (ns)	QY (%)
CdSe-4	0.08	3	2.2	8.08	4
CdSe-6.5	0.10	4	2.2	24.2	6.5
CdSe-8	0.13	4.5	2.2	27	8
CdSe-14	0.13	3 (ODA)	2.5	28.1	14
CdSe-16	0.076	2.8 (ODA)	1.5 (TBP)	29	16

The QYs of the CdSe cores and the core/shell NQDs are characterized using steady-state and time-resolved PL studies. In recent literature,[7] the relatively low QY in these thick-shell NQDs has been attributed to the presence of a high rate of nonradiative recombination through an Auger process,[29] and it is proposed that an effective means of reducing Auger recombination is to efficiently form an alloy layer at the interface to smoothen the potential. Here, in this study, we deliberately prepared 3 nm CdSe cores with a differing extent of surface defects by modifying the concentration of surface ligands.[32] The extent of surface defects was characterized by time-resolved fluorescence at the emission maxima (shown in the Supporting Information, Figure S2). The decrease in average lifetime is taken as a measure of the increase in the nonradiative decay channels and hence an increase in the number of surface defects, as shown for the case CdSe-4 to CdSe-16 in Table 1. The lifetime decay plots for the case of a less defective core (CdSe-8) and the core/shell structure obtained from this core (CdSe-8/CdS) is shown in Figure 1a, while the corresponding steady-state PL data are shown in the inset to the figure. From Figure 1a, it is evident that CdSe-8 nanocrystals show a nearly single-exponential decay, and the QYs of these cores were found to be ∼7−8%, while that in Figure 1b (CdSe-4) showed a large percentage of nonradiative decay channels as well as the <5% QY. This is not surprising because the CdSe-4 nanocrystals were made highly defective by purposely lowering the concentration of surface ligands. However, upon overcoating the material with a thick shell of CdS for both high and low surface-defective CdSe (respectively shown in Figure 1a and b), the QY increased to greater than 50% and unexpectedly >90%, respectively. Along with the earlier claims of interesting optical properties like high stability, reduced Auger recombination, and suppressed blinking, to our knowledge, this is the first claim to a near-unity QY in thick-shell CdSe-based QDs although a near-unity QY has been obtained for thinner-shell NQDs.[25] The advantages of thick-shell QDs, as will be shown later in the Letter, is clearly in being able to translate this efficiency into the device.

In order to verify the validity of the QY measurement, we excited the sample as well as a known dye, rhodamine-101 in ethanol (QY > 95%), with a 520 nm light and measured the QY using an integrating sphere. The results of this measurement are shown in the main panel of Figure 1c, while the photograph of this emission is shown in the inset. From the figure, it is evident that not only the brightness of the NQDs is similar to that of the dye, but for a similar absorption, the areas under the curve for the NQD and dye emission are identical, thus verifying the QY of this sample.

The variation of the QY as a function of shell thickness both for the surface-defective (CdSe-4) and smooth core (CdSe-8) is shown in Figure 1d, suggesting that the core with a lower concentration of ligands produces more efficient core/shell

dx.doi.org/10.1021/jz401958u | J. Phys. Chem. Lett. 2013, 4, 3544−3549

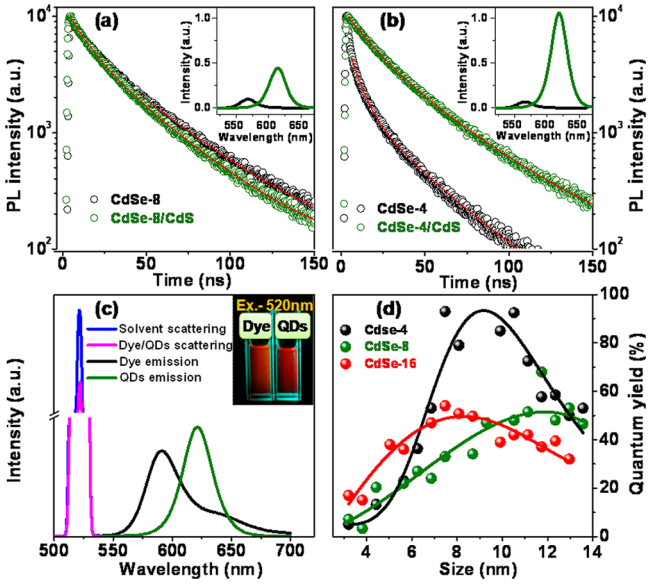

Figure 1. Engineering of the core−shell interface and its effect on the QY. The main panel shows the lifetime decay plots for CdSe-8 (a) and CdSe-4 (b) (black circles) and their corresponding core/shell structure (green circles). The red lines shows a biexponential fit to the corresponding data. The insets in both (a) and (b) shows the steady-state PL plots of these samples in relative units of QY, showing an increase in the QY of the core/shell structure upon comparison with the core. (c) The absolute QY of the sample as well as the rhodamine-101 dye obtained using integrating sphere measurements. The inset shows the photograph of the fluorescence of the dye as well as CdSe-4/CdS nanostructure obtained using excitation light of 520 nm showing similar brightness. (d) The variation of the QY as a function of shell thickness starting from three different cores with decreasing defects (CdSe-4 (black), CdSe-8 (green), CdSe-16 (red) (dots are experimental points, and the curves are a guide to the eye).

Table 2. Influence of Different CdSe Cores on Its Shell Formation

core	avg. lifetime of core (ns)	QY of the core (%)	avg. lifetime of core/shell (ns)	QY of core/shell (10.6 nm) (%)
CdSe-4	8.08	4	30.2	94
CdSe-8	27	8	26	60
CdSe-16	29	16	25.1	40

structures. Consistent with this surprising trend, as is seen from the compiled results in Table 2, CdSe-16, which had a highest QY of 16%, produced a rather low QY of 40% when overcoated with thick CdS shell material. In addition, it is also interesting to note that the QY increases with the increasing thickness of the shell material followed by a decrease. This is not surprising given that the PL QY is a complex interplay between various ligands. This is already evident in Figure 1d where the QY peaked at about 7.5 nm when the ligands tributylphosphine and octadecyl amine were used, while this was shifted to much higher sizes upon the use of appropriate amounts of trioctylphosphine, trioctylphosphine oxide, and oleylamine. In fact, our own studies have shown that with different shell overcoating procedures, we can only reach a maximum of 30% QY by varying the concentration of the ligands. This has been already studied in recent literature,[24,26] and the optimal concentrations of the ligands have been obtained. However, the most counterintuitive observation that is so far not explained is the high QY of the core/shell structure starting from low QY cores despite exactly similar overcoating procedures with identical ligands. In order to understand these unforeseen results, we performed a study of the microstructure to explore the interfacial defects and correlate their physical properties to these defects.

Though low PL efficiency in the presence of surface defects is well-documented and it is well-known that large lattice mismatch between the core and the shell material is instrumental for the absence of improvement in PL efficiency, the effect of a sharp interface in the presence of a rather low lattice mismatch of 3.9% on the PL efficiency has not been studied until now.

While it is not possible to microscopically observe structural defects at the surface, the consequences of surface defects would be easily visible when overcoated with a thin CdS layer. When CdS is overcoated on a highly surface defective core, the random direction of the defects is reflected even after overcoating, giving rise to internal defects radiating in random directions. However, when the surface is relatively smooth, we observe only a unidirectional defect at the interface of the core and shell. The high-resolution image of the two-monolayer CdS-overcoated material obtained from the low surface defective core (CdSe-8) is observed to have a large percentage of nanostructures characterized by line defects along one single direction, as shown by the red arrows in Figure 2a. On the

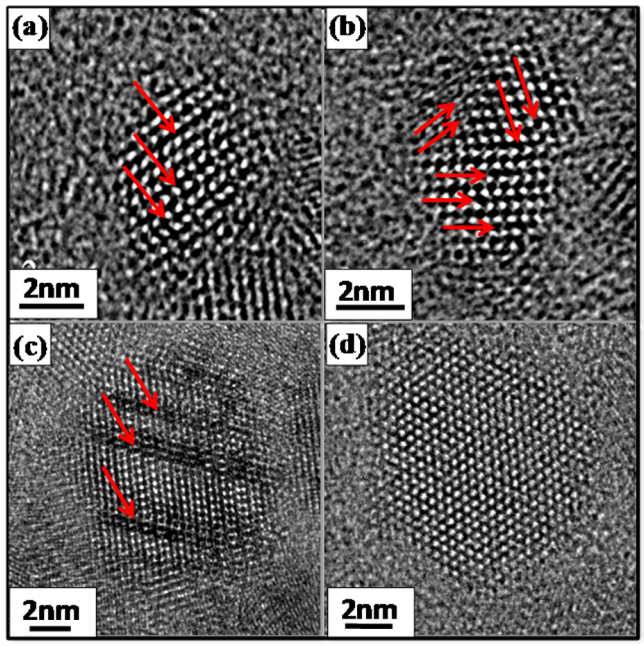

Figure 2. Study of defects. The high-resolution TEM images of (a) CdSe-8/2 ML CdS showing interface defects, (b) CdSe-4/2 ML CdS showing defects in random directions, (c) CdSe-8/12 ML CdS showing interface defects, and (d) CdSe-4/12 ML CdS showing a perfect defect-free crystal. Defects are shown by red arrows.

other hand, the HRTEM image obtained after overcoating two monolayers of CdS on a surface-defective core (CdSe-4) shows defects radiating in random directions, as shown by the red arrows (Figure 2b). Not surprisingly, the line defects present in the case of CdSe-8 shown in Figure 2a were retained despite further overcoating with a thick shell of CdS followed by annealing, as shown by the image in Figure 2c. However, a similar procedure carried out for the case of CdSe-4 shown in Figure 2b amazingly shows that most of the NQDs were found

dx.doi.org/10.1021/jz401958u | J. Phys. Chem. Lett. 2013, 4, 3544−3549

to be perfectly defect-free, as shown in Figure 2d. In order to make sure that this is not just an anomaly but indeed the statistical trend, we performed a defect analysis on 350−400 particles. HRTEM images of these nanocrystals showing a larger number of nanocrystals as well as the defects (shown by red arrows) are given in the Supporting Information (S3−S6). Further, an analysis of the HRTEM images as a function of shell thickness (shown in Supporting Information, Figure S7 and Table S1) shows that the defects indeed are annealed out, paving the way for the increase in the QY as a function of shell thickness as well. Thus, both of the observations in Figure 1d can be explained by studying the microstructure. However, though the microstructure is shown to dictate the PL QY in these materials, it is known that obtaining a defect-free crystal is a delicate balance between long annealing time at high temperature and optimal retention of the ligands on the surface at these high temperatures.

From a fundamental perspective, though the results discussed above prove that the defect-free NQDs give a near-unity QY, the defective particles may either be completely "dark" or have a lower than unity QY. A direct correlation of defects with the QY of the sample with similar shell thicknesses but with a different number of defective particles may be expected to provide more insight into this fundamental issue. Accordingly, we used the different CdSe 3 nm cores defined in Table1 and overcoated them with a CdS shell to obtain a total size of about 8.5 ± 1 nm particles. The results of this study are summarized in various panels of Figure 3 and in Table 3. The panels of Figure 3a−d show the typical HRTEM images of samples obtained from thick-shell samples with differing defective particles (CdSe-14, CdSe-16, CdSe-8, and CdSe-4, respectively). The size and size distribution obtained from the analysis of about 300−350 particles in every case are shown in the corresponding insets. The percentage of size distribution in all

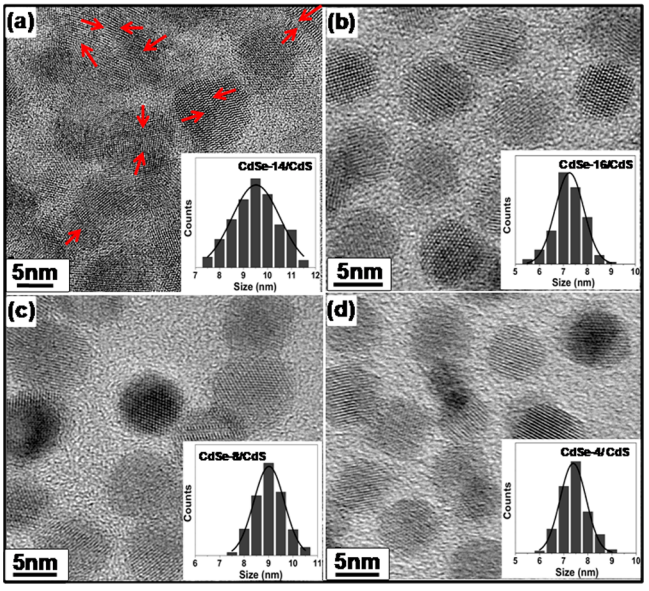

Figure 3. Nanostructure characterization using high-resolution TEM. High-resolution TEM images showing the formation of defective and nondefective thick-shell core/shell nanostructures for (a) CdSe-14/CdS, (b) CdSe16/CdS, (c) CdSe-8/CdS, and (d) CdSe-4/CdS. Red arrows in (a) point to the directions of the defects. The insets show the size distribution histogram obtained by measuring the sizes of about 300−400 nanostructures.

Table 3. Various Sizes, Size Distributions, Percentages of Nondefective Particles, As Well As the QY for the Particles Found in Panels (a−d) in Figure 3

panel	(a)	(b)	(c)	(d)
core	CdSe-14	CdSe-16	CdSe-8	CdSe-4
core/shell size (nm)	9.5	7.5	9	8
size distribution (%)	10.5	8.1	7	7.4
nondefective particles (%)	58.5	75	79	86
QY (%)	8	40	60	94

cases is found to be below 10% and mostly spherical particles. The percentage size distribution as well as the number of defective particles and the QY of the sample are tabulated in Table 3. Similar to the studies discussed earlier, the extent of surface defects, as quantified by the percentage of nonradiative decay, was proportional to the number of defective particles. CdSe-14 was overcoated using a slightly different overcoating procedure, resulting in particles with defects along different directions, as seen in the HRTEM image in Figure 3a. This is indicative of low crystallinity of the nanostructure that is also reflected in the extremely low QY (~8%) of these samples. Nevertheless, more interestingly, from Table 3 as well as the graph shown in the Supporting Information, Figure S8, it appears that though the particles have almost the same size core and shell, with a small decrease in the percentage of defective particles, we observe a rather large change in the QY of the samples. While this information seems indicative of not completely dark defective particle, this cannot be assumed to be completely convincing. Statistically, only about 27% of defective particles are normally in the right orientation to observe these defects. With small changes like 25−20% defective particles, as observed from our data here, due to the statistical error bar, it would be difficult to exactly estimate the number of defective structures, and hence, a direct quantitative correlation to the QY is not possible. Thus, from our analysis of the emission properties, we show that the defects of different types form a major contribution to the quenching of the QY, although it is known that the QY is a convoluted response of various factors. The defect-free core/shell NQDs obtained from a surface-defective core have been shown for the first time to have a highly stable, near-unity QY, despite their wurtzite crystal structure.

These high QY materials, combined with the low Auger recombination rate that has already been shown in the literature for these samples,[13] present substantial improvements over the commercially available nanocrystals. Since the discovery of high QY, narrow band emission of NQDs, these materials have been explored for the possibility of use as an active layer in LEDs. However, nanocrystal charging under LED operation renders NQDs optically inactive, consequently reducing the efficiency of these devices. Recently, it has been shown that these thick-shell NQDs, even with only 10−20% QY, are quite efficient in LEDs.[21] Our materials retain all of the previously observed advantages along with near-unity QY. Specifically, the stability of the PL quantum efficiency under intense UV radiation light is shown in Figure S9 of the Supporting Information.

Hence, in order to translate the QY into device efficiency, we fabricated simple architecture proof-of-concept LED devices using these NQDs with different QYs (shown in Figure 4) as the active layer. The device architecture used in these devices is shown in Figure 4a. The poly (3-hexyl thiophene) (P3HT) layer, introduced as a hole-transport layer[33] (as shown from

dx.doi.org/10.1021/jz401958u | J. Phys. Chem. Lett. 2013, 4, 3544−3549

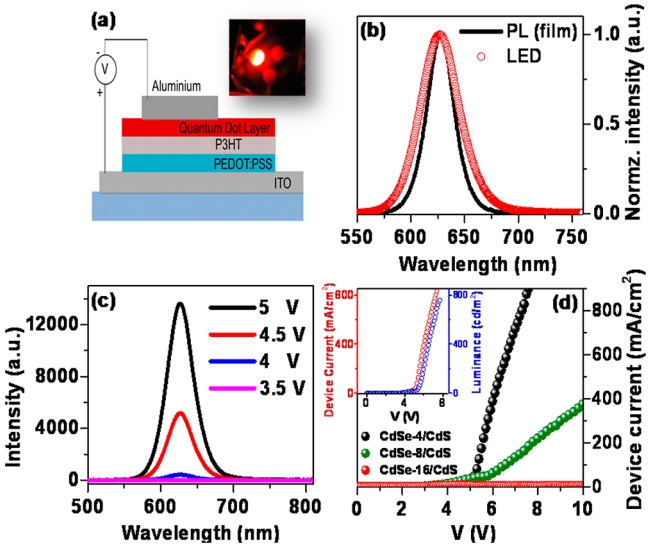

Figure 4. LED characterization. (a) The schematic of the device architecture. The inset shows the photograph of the LED under operation. (b) Spectral profile of the LED device and comparison with the PL of the QD film on glass. (c) LED emission spectrum with various driving voltages. (d) $J-V$ characteristics of devices obtained from 40% (CdSe-16) and 60% (CdSe-8) QY materials in comparison with that of near-unity QY (CdSe-4) materials. The maximum luminance output from the 60% sample was ~20 Cd/m^2, and the luminance from the 40% sample was very low. The inset shows typical $J-V$ characteristics for the 94% QY sample (CdSe-4/CdS) and emission intensity as a function of the bias for the ITO|PEDOT-PSS|P3HT|QD|Al device.

band offsets in Supporting Information, Figure S10), assisted in the decrease of the threshold voltage from >8 to ~3 V with no change in the spectral characteristics but a substantial increase in the emission magnitude and stability. Emission from a typical device is shown in the inset to Figure 4a. The emission band obtained from electroluminescence (EL) was identical to that obtained from PL and was centered at 628 nm with a full width at half-maximum (fwhm) < 45 nm (Figure 4b). This equivalence of PL and EL emission indicates a common excitonic origin with the NQD layer as the source of emission. All of the devices tested in this device configuration exhibited light emission, and the emission flux showed linear dependence with the current density. The emission wavelength remains unchanged at higher intensities as the bias voltage is increased (Figure 4c). The current density versus voltage ($J(V)$) characteristics of these NQD-based active layer devices are shown in the inset to Figure 4d and exhibited typical diode characteristics. It was possible to drive some devices to 9 V with an injection current density of 0.3 A/cm^2 to result in emission exceeding 7000 Cd/m^2. Similar devices made out of lower QY materials of identical composition were highly unstable and inefficient, as shown in the main panel of Figure 4d. These trends in our observations point out that the improvement in PL yields is translatable to the LED attributes. It should be pointed out that a very simple device obtained using the near-unity QDs shown in this work with no state of the art, trial and error processes has shown high efficiency in every device that has been tried in our laboratory so far. That is a remarkable achievement in the field of nanocrystal/organic-electronics and cannot be simply achieved with a thin coating of CdS shell,[25] though the QY can be close to unity. Further optimization of the device with a choice of different thickness of the active layers, hole-injecting layers, and cathodes would be expected to yield improved device characteristics.

Thus, in conclusion, we have shown for the first time that the QY of the NQDs is highly sensitive to crystal structure defects within the NQDs and that a near-unity QY can be obtained by synthesizing defect-free nanostructures. This also establishes the relationship between the quality of the microstructure and electronic properties of the NQDs. We have also shown that these defect-free core/shell structures with a smooth alloy interface can be obtained quite counterintuitively, using cores that are highly surface defective. From a fundamental perspective, we have studied the role of defective particles in emission and find that the defect density and direction determine the efficiency of the emission. These high QY NQDs have been used as an active layer in fabricating a proof-of-concept LED device that is shown to be quite efficient, in fact, comparable with the organic–nanocrystal hybrid device efficiencies.

■ ASSOCIATED CONTENT

Supporting Information

Experimental methods, characterizations, time-resolved fluorescence, high-resolution TEM, variation of the QY as a function of the number of defects, stability of the quantum efficiency, and band offsets. This material is available free of charge via the Internet at http://pubs.acs.org.

■ AUTHOR INFORMATION

Corresponding Author

*E-mail: rv@jncasr.ac.in.

Notes

The authors declare no competing financial interest.

■ ACKNOWLEDGMENTS

We thank JNCASR, Sheikh Saqr Laboratory, and the Department of Science and Technology, Government of India for financial support. A.S. thanks CSIR for a research fellowship.

■ REFERENCES

(1) Hoy, J.; Morrison, P. J.; Steinberg, L. K.; Buhro, W. E.; Loomis, R. A. Excitation Energy Dependence of the Photoluminescence Quantum Yields of Core and Core/Shell Quantum Dots. *J. Phys. Chem. Lett.* **2013**, *4*, 2053–2060.

(2) Frederick, M. T.; Amin, V. A.; Weiss, E. A. Optical Properties of Strongly Coupled Quantum Dot Ligand Systems. *J. Phys. Chem. Lett.* **2013**, *4*, 634–640.

(3) Klimov, V. I.; Ivanov, S. A.; Nanda, J.; Achermann, M.; Bezel, I.; McGuire, J. A.; Piryatinski, A. Single-Exciton Optical Gain in Semiconductor Nanocrystals. *Nature* **2007**, *447*, 441–446.

(4) Aldeek, F.; Balan, L.; Medjahdi, G.; Roques-Carmes, T.; Malval, J.-P.; Mustin, C.; Ghanbaja, J.; Schneider, R. Enhanced Optical Properties of Core/Shell/Shell CdTe/CdS/ZnO Quantum Dots Prepared in Aqueous Solution. *J. Phys. Chem. C* **2009**, *113*, 19458–19467.

(5) Peng, X.; Schlamp, M. C.; Kadavanich, A. V.; Alivisatos, A. P. Epitaxial Growth of Highly Luminescent CdSe/CdS Core/Shell Nanocrystals with Photostability and Electronic Accessibility. *J. Am. Chem. Soc.* **1997**, *119*, 7019–7029.

(6) She, C.; Demortiere, A.; Shevchenko, E. V.; Pelton, M. Using Shape to Control Photoluminescence from CdSe/CdS Core/Shell Nanorods. *J. Phys. Chem. Lett.* **2011**, *2*, 1469–1475.

(7) Gomez-Campos, F. M.; Califano, M. Hole Surface Trapping in CdSe Nanocrystals: Dynamics, Rate Fluctuations, and Implications for Blinking. *Nano Lett.* **2012**, *12*, 4508−4517.
(8) Eijt, S. W. H.; van Veen, A. T.; Schut, H.; Mijnarends, P. E.; Denison, A. B.; Barbiellini, B.; Bansil, A. Study of Colloidal Quantum-Dot Surfaces Using an Innovative Thin-Film Positron 2D-ACAR Method. *Nat. Mater.* **2005**, *5*, 23−26.
(9) Hoy, J.; Morrison, P. J.; Steinberg, L. K.; Buhro, W. E.; Loomis, R. A. Excitation Energy Dependence of the Photoluminescence Quantum Yields of Core and Core/Shell Quantum Dots. *J. Phys. Chem. Lett.* **2013**, *4*, 2053−2060.
(10) Becerra, L. R.; Murray, C. B.; Griffin, R. G.; Bawendi, M. G. Investigation of the Surface Morphology of Capped CdSe Nanocrystallites by ^{31}P Nuclear Magnetic Resonance. *J. Chem. Phys.* **1994**, *100*, 3297−3300.
(11) McBride, J.; Treadway, J.; Feldman, L. C.; Pennycook, S. J.; Rosenthal, S. J. Structural Basis for Near Unity Quantum Yield Core/Shell Nanostructures. *Nano Lett.* **2006**, *6*, 1496−1501.
(12) Chen, Y.; Vela, J.; Htoon, H.; Casson, J.; Werder, D.; Bussian, D.; Klimov, V.; Hollingsworth, J. "Giant" Multishell CdSe Nanocrystal Quantum Dots with Suppressed Blinking. *J. Am. Chem. Soc.* **2008**, *130*, 5026−5027.
(13) García-Santamaría, F.; Brovelli, S.; Viswanatha, R.; Hollingsworth, J. A.; Htoon, H.; Crooker, S. A.; Klimov, V. I. Breakdown of Volume Scaling in Auger Recombination in CdSe/CdS Heteronanocrystals: The Role of the Core−Shell Interface. *Nano Lett.* **2011**, *11*, 687−693.
(14) Brovelli, S.; Schaller, R. D.; Crooker, S. A.; Garcia-Santamaria, F.; Chen, Y.; Viswanatha, R.; Hollingsworth, J. A.; Htoon, H.; Klimov, V. I. New Paradigm for Controlling Exciton Dynamics via Engineered Electron−Hole Exchange Interaction. *Nat. Commun.* **2011**, *2*, 280.
(15) Mahler, B.; Spinicelli, P.; Buil, S.; Quelin, X.; Hermier, J. P.; Dubertret, B. Towards Non-Blinking Colloidal Quantum Dots. *Nat. Mater.* **2008**, *7*, 659−664.
(16) Spinicelli, P.; Buil, S.; Quelin, X.; Mahler, B.; Dubertret, B.; Hermier, J. P. Bright and Grey States in CdSe−CdS Nanocrystals Exhibiting Strongly Reduced Blinking. *Phys. Rev. Lett.* **2009**, *102*, 136801.
(17) Garcia-Santamaria, F.; Chen, Y.; Vela, J.; Schaller, R. D.; Hollingsworth, J. A.; Klimov, V. I. Suppressed Auger Recombination in "Giant" Nanocrystals Boosts Optical Gain Performance. *Nano Lett.* **2009**, *9*, 3482−3488.
(18) Fu, Y.; Zhou, Y. H.; Su, H.; Boey, F. Y. C.; Agren, H. Impact Ionization and Auger Recombination Rates in Semiconductor Quantum Dots. *J. Phys. Chem. C* **2010**, *114*, 3743−3747.
(19) Park, Y. S.; Malko, A. V.; Vela, J.; Chen, Y.; Ghosh, Y.; Garcia-Santamaria, F.; Hollingsworth, J. A.; Klimov, V. I.; Htoon, H. Near-Unity Quantum Yields of Biexciton Emission from CdSe/CdS Nanocrystals Measured Using Single-Particle Spectroscopy. *Phys. Rev. Lett.* **2011**, *106*, 187401.
(20) Krauss, T. D.; Peterson, J. J. Bright Future for Fluorescence Blinking in Semiconductor Nanocrystals. *J. Phys. Chem. Lett.* **2010**, *1*, 1377−1382.
(21) Pal, B. N.; Ghosh, Y.; Brovelli, S.; Laocharoensuk, R.; Klimov, V. I.; Hollingsworth, J. A.; Htoon, H. "Giant" CdSe/CdS Core/Shell Nanocrystal Quantum Dots As Efficient Electroluminescent Materials: Strong Influence of Shell Thickness on Light-Emitting Diode Performance. *Nano Lett.* **2012**, *12*, 331−336.
(22) Kundu, J.; Ghosh, Y.; Dennis, A. M.; Htoon, H.; Hollingsworth, J. A. Giant Nanocrystal Quantum Dots: Stable Down-Conversion Phosphors that Exploit a Large Stokes Shift and Efficient Shell-to-Core Energy Relaxation. *Nano Lett.* **2012**, *12*, 3031−3037.
(23) Lin, C. C.; Liu, R.-S. Advances in Phosphors for Light-Emitting Diodes. *J. Phys. Chem. Lett.* **2011**, *2*, 1268−1277.
(24) Ghosh, Y.; Mangum, B. D.; Casson, J. L.; Williams, D. J.; Htoon, H.; Hollingsworth, J. A. New Insights into the Complexities of Shell Growth and the Strong Influence of Particle Volume in Nonblinking "Giant" Core/Shell Nanocrystal Quantum Dots. *J. Am. Chem. Soc.* **2012**, *134*, 9634−9643.
(25) Chen, O.; Zhao, J.; Chauhan, V. P.; Cui, J.; Wong, C.; Harris, D. K.; Wei, H.; Han, H.-S.; Fukumura, D.; Jain, R. K.; Bawendi, M. G. Compact High-Quality CdSe−CdS Core−Shell Nanocrystals with Narrow Emission Linewidths and Suppressed Blinking. *Nat. Mater.* **2013**, *12*, 445−451.
(26) Nan, W.; Niu, Y.; Qin, H.; Cui, F.; Yang, Y.; Lai, R.; Lin, W.; Peng, X. Crystal Structure Control of Zinc-Blende CdSe/CdS Core/Shell Nanocrystals: Synthesis and Structure-Dependent Optical Properties. *J. Am. Chem. Soc.* **2012**, *134*, 19685−19693.
(27) Cragg, G. E.; Efros, A. L. Suppression of Auger Processes in Confined Structures. *Nano Lett.* **2009**, *10*, 313−317.
(28) Wang, X.; Ren, X.; Kahen, K.; Hahn, M. A.; Rajeswaran, M.; Maccagnano-Zacher, S.; Silcox, J.; Cragg, G. E.; Efros, A. L.; Krauss, T. D. Non-Blinking Semiconductor Nanocrystals. *Nature* **2009**, *459*, 686−689.
(29) Efros, A. L. Nanocrystals: Almost Always Bright. *Nat. Mater.* **2008**, *7*, 612−613.
(30) Cho, K. S.; Lee, E. K.; Joo, W. J.; Jang, E.; Kim, T. H.; Lee, S. J.; Kwon, S. J.; Han, J. Y.; Kim, B. K.; Choi, B. L. High-Performance Crosslinked Colloidal Quantum-Dot Light-Emitting Diodes. *Nat. Photonics* **2009**, *3*, 341−345.
(31) Kim, T. H.; Cho, K. S.; Lee, E. K.; Lee, S. J.; Chae, J.; Kim, J. W.; Kwon, J. Y.; Amaratunga, G.; Lee, S. Y.; Choi, B. L. Full-Colour Quantum Dot Displays Fabricated by Transfer Printing. *Nat. Photonics* **2011**, *5*, 176−182.
(32) Ning, Z.; Molnar, M.; Chen, Y.; Friberg, P.; Gan, L.; Agren, H.; Fu, Y. Role of Surface Ligands in Optical Properties of Colloidal CdSe/CdS Quantum Dots. *Phys. Chem. Chem. Phys.* **2011**, *13*, 5848−5854.
(33) Zhao, J.; Bardecker, J. A.; Munro, A. M.; Liu, M. S.; Niu, Y.; Ding, I. K.; Luo, J.; Chen, B.; Jen, A. K. Y.; Ginger, D. S. Efficient CdSe/CdS Quantum Dot Light-Emitting Diodes Using a Thermally Polymerized Hole Transport Layer. *Nano Lett.* **2006**, *6*, 463−467.